AIAA-2000-1437

VALIDATION OF STRUCTURAL DYNAMICS MODELS AT LOS ALAMOS NATIONAL LABORATORY

François M. Hemez[*] and Scott W. Doebling[†]
Engineering Analysis Group (ESA-EA)
Los Alamos National Laboratory
P.O. Box 1663, M/S P946
Los Alamos, New Mexico 87545

ABSTRACT

This publication proposes a discussion of the general problem of validating numerical models for nonlinear, transient dynamics. The predictive quality of a numerical model is generally assessed by comparing the computed response to test data. If the correlation is not satisfactory, an inverse problem must be formulated and solved to identify the sources of discrepancy between test and analysis data. Some of the most recent work summarized in this publication has focused on developing test-analysis correlation and inverse problem solving capabilities for nonlinear vibrations. Among the difficulties encountered, we cite the necessity to satisfy continuity of the response when several finite element optimizations are successively carried out and the need to propagate variability throughout the optimization of the model's parameters. After a brief discussion of the formulation of inverse problems for nonlinear dynamics, the general principles which, we believe, should guide future developments of inverse problem solving are discussed. In particular, it is proposed to replace the resolution of an inverse problem with multiple forward, stochastic problems. The issue of defining an adequate metrics for test-analysis correlation is also addressed. Our approach is illustrated using data from a nonlinear vibration testbed and an impact experiment both conducted at Los Alamos National Laboratory in support of the advanced strategic computing initiative and our code validation and verification program.

1. INTRODUCTION

Advances in computational and modeling capabilities make it possible to simulate a wide range of difficult problems that would have been off-limits just a few decades ago. However, developing models and obtaining numerical solutions do not necessarily imply that the resulting predictions are correct. Weather forecast, prediction of acoustic levels and reliability analysis of mechanical systems are a few examples that illustrate this difficulty on a daily basis.

This work addresses the general problem of model validation, that is, how to assess the predictive accuracy of a numerical simulation and its ability to capture the dynamics or physics of interest. Model validation includes classes of problems that have been and continue to be extensively studied among which we cite health monitoring, damage detection and finite element model updating. All these have in common the need to fit a parametrized model to a reference solution or test data, therefore, defining an inverse problem. Some of the general principles which, we believe, should guide the development of inverse problem solving for the 21st century, are discussed. These include the development of general-purpose, nonlinear models; the analysis of transient, time-domain data; greater imagination in feature extraction and the definition of test-analysis metrics; dedicated numerical analysis tools for increasing the efficiency of inverse problem solving; decentralized measurement and computational strategies; the propagation of variability information during the direct and inverse calculations; and the formulation of statistical, hypothesis testing to assess the consistency between test data and multiple numerical simulations.

Some aspects of this "philosophy" are illustrated using nonlinear vibration data and an impact experiment designed for characterizing the behavior of a highly nonlinear hyperelastic material. Various metrics for test-analysis correlation are compared, response surfaces are defined to optimize the design parameters and fast probability integration is used for assessing the consistency of various models with respect to test data in a statistical sense.

2. MOTIVATION

The main reason why numerical models have become so popular is because it is much less expensive to use computational time than it is to run a sophisticated experiment. Many practical situations also occur where the phenomenon of interest can not be measured directly. For example, this is the case with large space antennas developed for observation and communication purposes that do not withstand their own weight in an environment of 1-g of gravity. So, the analyst must rely on numerical simulations to establish the dynamic characteristics of the structure and to validate control laws.[1] Another example is the diagnosis of cracks or faulty mechanical components in civil engineering structures or airplanes. In this case, testing methodologies are simply not yet available due to the complexity of such systems and engineers must rely on localized screening or component testing, which turns out to be time-consuming and very expensive. Modal testing-based health monitoring appears to be a promising alternative.[2] Hence, the scientific community has turned to numerical models that can be parametrized and used to study a wide variety of situations.

This argument has been reinforced in recent years by the increasing efficiency of processors, the greater availability of memory, the breakthrough of object-oriented data structures together with the growing popularity of parallel processing whether it involves computers with massively parallel architectures or networks of single-CPU workstations. Interestingly enough, the miniaturization of CPU's and their greater efficiency have influenced greatly testing procedures, making it possible to instrument structures with hundreds of transducers. Powerful data analysis and friendly computer graphics are also a driving force behind the development of non-intrusive, optical measurement systems such as holography and laser vibrometry. These technological breakthroughs are not without major consequences on the way engineers are analyzing structural systems today and on their

conception of test-analysis correlation and inverse problem solving. In the first case, an illustration is the rapid development of modeling and computational procedures for nonlinear dynamics. In the second case, modal-based updating techniques developed originally to refine linear structural dynamics models are evolving into the broader notion of model validation. This work defines and explores this last concept.

The articulation between testing, modeling and inverse problem solving is illustrated in Figure 1 where arrows represent the flow of information. Here, inverse problem solving is replaced by a methodology where response surfaces are generated from the resolution of a large number of forward analyses. This best utilizes our capabilities for modeling nonlinear systems and our parallel processing resources. Two other important contributions to this work are 1) the ability to derive high accuracy, physics-based material models and 2) fast probability integration for large-scale structural analysis. The first one is not discussed in this paper but it is briefly mentioned because physics-based models of material behavior are generally obtained from a microscopic description of the material. As such, they depend on parameters that can not be measured with great accuracy and that are best characterized by probabilistic distributions. This explains why fast probability integration techniques are critical to our work and why optimization algorithms are required, not only to adjust parameters of the models, but also to assess the quality of models in a probabilistic sense.
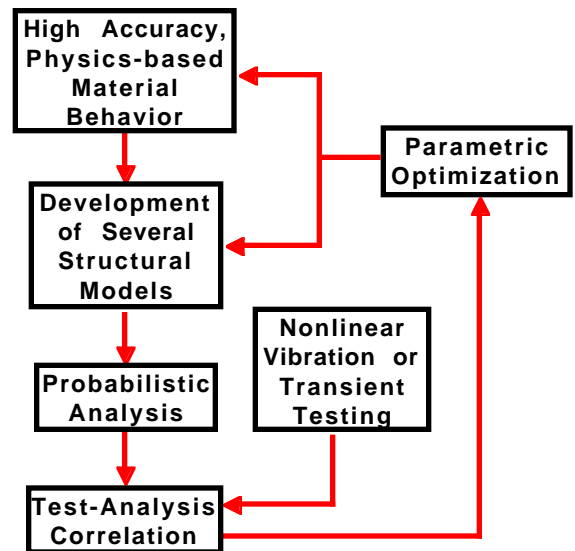
Figure 1. Flow chart describing the different steps of testing, modeling, analysis and validation.

American Institute of Aeronautics and Astronautics

3. DESCRIPTION OF LANL TESTBEDS FOR MODEL VALIDATION

To illustrate our views of model validation, two experiments performed at Los Alamos National Laboratory (LANL) are briefly described. The first testbed is a eight-degree of freedom vibrating system that exhibits significant friction and nonlinear oscillations. The purpose of the second testbed is to characterize the behavior of an elastomeric layer of material subjected to a short-duration impact. Both experiments are designed to provide test data that can be studied to quantify the variability of a component-level experiment and to assess the adequacy of our model validation procedures.

3.1. TESTBED FOR NONLINEAR VIBRATIONS

Our testbed for the validation of nonlinear vibration modeling is the LANL 8-DOF system (which stands for Los Alamos National Laboratory eight degrees of freedom) illustrated in Figure 2. It consists of eight masses connected by linear springs. The masses are free to slide along a center rod that provides support for the whole system. Modal tests are performed on the nominal system and on a damaged version where the stiffness of various springs is reduced by 14% or 24%. The exercise consists in identifying the location and extent of structural damage by optimizing the spring stiffness of each spring of the numerical model. This procedure illustrates the conventional approach to model updating where test-analysis correlation requires the definition of modal-based features such as, for example, the difference between identified and predicted frequencies or the modal assurance criterion (MAC) formed between test and analysis mode shapes. Obviously, this approach is justified for linear models when the dynamics is dominated by the system's low frequency modes.
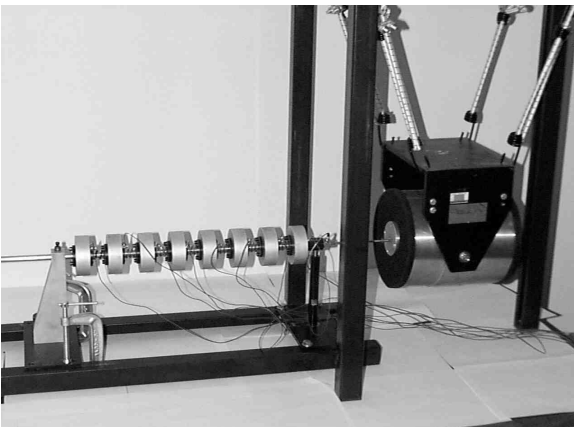
Figure 2. LANL 8-DOF testbed.

Even though the original, linear model is in good agreement with the measured modal parameters, friction introduces an unambiguous nonlinearity in the system's response as shown in Figures 3 and 4. They represent the changes in identified modal frequencies (Figure 3) and damping ratios (Figure 4) as the level of force used to excite the system is increased.
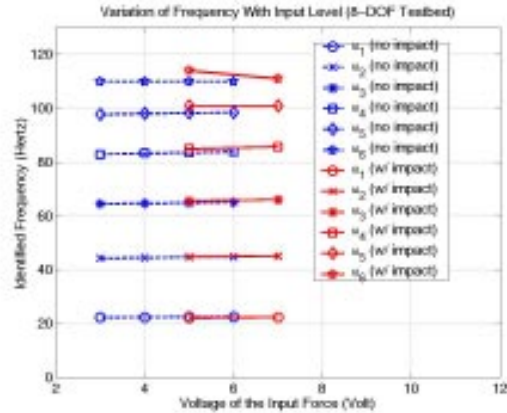
Figure 3. Evolution of modal frequencies identified with the 8-DOF testbed as the input level is increased.
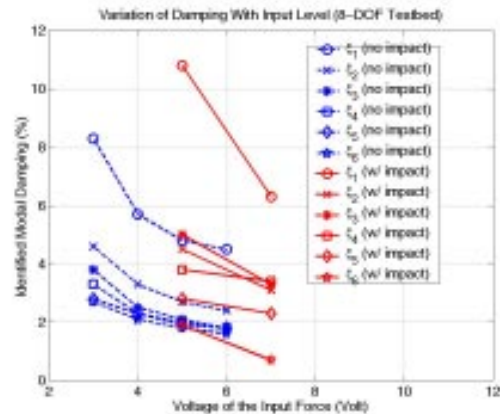
Figure 4. Evolution of damping ratios identified with the 8-DOF testbed as the input level is increased.

Frequencies do not vary significantly because the distribution of mass and stiffness is unchanged. The amount of damping in the system, however, is overall reduced because higher forcing levels tend to reduce the "stick and slip" phenomenon. As a result, our attempts to identify the damage based on conventional model updating techniques fail as long as friction is not accounted for in the numerical model.[3,4] An important conclusion is that modal parameters, although popular and widely used in the community of modal analysis, may not be the best indicators when it comes to assessing the dynamics of a system.

A contact mechanism can also added between two masses to induce a source of contact/impact. It is pictured in Figure 5. When the system is used in this nonlinear mode, acceleration data are measured at each one of the eight masses. Then, features extracted from the time series can be compared to their numerical counterparts to assess the predictive quality of a particular model or family of models. Examples of such features are, again, the modal parameters identified from the measurements. They can also be defined using the difference of time series, polynomial fits, principal component decomposition, etc.

Figure 5. Contact mechanism of the LANL 8-DOF testbed for nonlinear vibrations.
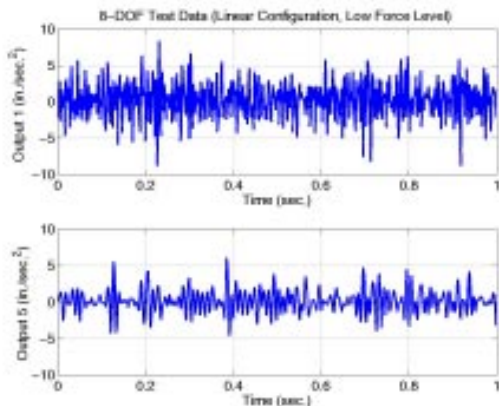
Figure 6. Accelerations measured at sensor 1 (top) and sensor 5 (bottom) for the LANL 8-DOF testbed.

Figure 6 illustrates the raw test data. Accelerations measured at locations 1 and 5 are shown when the system is configured with the impact mechanism and excited by a random signal at location 1. Several examples of features such as those mentioned previously are given and their ability to discriminate "good" models

from "poor" models is illustrated in Section 5.3. This issue is critical because the transient oscillations featured by these data make it difficult to establish a comparison based, for example, on the root mean square (RMS) error between measured and predicted time series.

With the nonlinear configuration, the test we are interested in is two-fold. First, the best possible friction model must be obtained. Then, the ability of inverse problem solving to identify a damaged spring and to discriminate between structural damage and impact nonlinearity is investigated. This is achieved by building a parametric, explicit finite element model of the system; generating the time-domain responses; and minimizing the "distance" between test data and predictions, whether the distance is evaluated in the time or frequency domain. This optimization problem can be formulated as the minimization of the cost function shown in equation (1) where the first contribution represents the metric used for test-analysis correlation and the second contribution serves the purpose of regularization and promotes minimum-change solutions

$$\min_{\{\delta p\}} \sum_{j=1\cdots N_{test}} \left\{R_j(p+\delta p)\right\}^* \left[S_{RR_j}\right]^{-1} \left\{R_j(p+\delta p)\right\}$$
$$+\left\{\delta p\right\}^T \left[S_{pp}\right]^{-1} \left\{\delta p\right\} \tag{1}$$

Constraints such as $p_{min} \leq (p_e + \delta p_e) \leq p_{max}$ are added to the formulation to eliminate any local minimum that would not be acceptable from a physical standpoint. The weighting matrices in equation (1) are generally kept constant and diagonal for computational efficiency. They can also be defined as general covariance matrices which then formulates a Bayesian correction procedure.[5]

3.2. TESTBED FOR TRANSIENT IMPACT

The purpose of this experiment is to provide us with test data that can be used for validating the predictive quality of a numerical model based on explicit finite element (FE) simulations. The application targeted is a high-frequency shock test that features a component characterized by a nonlinear, viscoelastic material. Major differences compared to the previous 8-DOF system are the dynamics observed (transient as opposed to nonlinear vibrations); the larger computational effort required to simulate the response (the numerical model consists of several thousand degrees of freedom and Lagrange multipliers); and the need to develop stochastic models that account for sources of variability and uncertainty.

3.2.1. Numerical Modeling

The setup is illustrated in Figure 7. It can be observed that the main two components (steel impactor and foam layer) are assembled on a mounting plate that is attached to the carriage. The center of the steel cylinder is hollow and it is fixed with a rigid collar to restrict the motion of the impactor to the vertical direction. This assures perfectly bilinear contact between the steel and foam components, allowing the structure to be modeled axi-symmetrically. In spite of this, a full three-dimensional model is also developed to verify this assumption's validity.
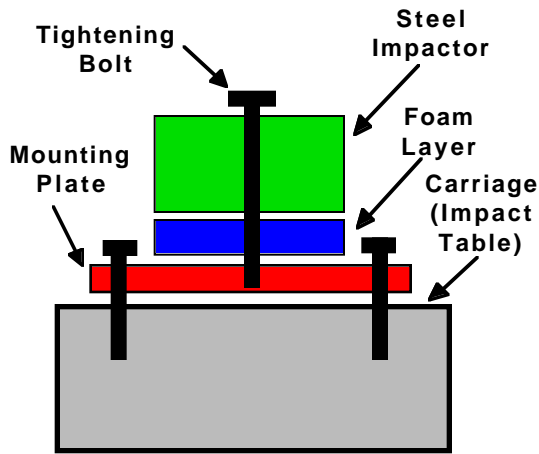
Figure 7. Description of the assembly of the cylindrical impactor and carriage.
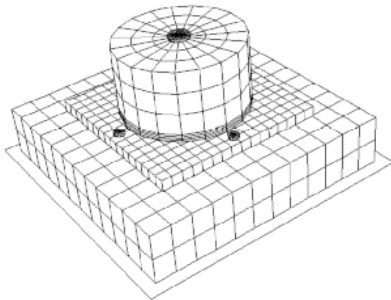
Figure 8. 3D model of the impact testbed.

Figure 8 illustrates one of the discretized models developed for numerical simulation. The analysis program used for these calculations is HKS/Abaqus-Explicit, a general-purpose package for finite element modeling of nonlinear structural dynamics.[6] It features an explicit time integration algorithm, which is convenient when dealing with nonlinear materials, impact or contact, and high frequency excitations.

In an effort to match the test data, several FE models are developed by varying, among other things, the constitutive law and the type of modeling. Therefore, optimization variables consist of the usual design variables augmented with structural form parameters such as kinematic assumptions, geometry description (2D or 3D), contact modeling and numerical viscosity. Another important parameter is the amount of preload applied by the bolt used to hold this assembly together. The torque applied was not measured during testing and it may have varied from test to test. The resulting difficulty is that the amount of preload applied must be considered a random variable because it is believed to have contributed to the variability of the experiment. By opposition, variables describing the material are unknown but deterministic because they do not vary as long as the same sample of material is tested. This implies that the analysis tools must be able to handle random variables and test-analysis correlation must be recast into a more general stochastic framework.

3.2.2. Experiment Setup

During the actual test, the carriage that weights 955 lbm (433 kg) is dropped from various heights and impacts a rigid floor.[7] The input acceleration is measured on the top surface of the carriage and three output accelerations are measured on top of the steel impactor that weights 24 lbm (11 kg). Figure 9 provides an illustration of the test setup and instrumentation. This impact test is repeated several times to collect multiple data sets from which the experiment's repeatability can be assessed. At impact, the steel cylinder compresses the foam to cause elastic and plastic strains during a few micro-seconds as shown in Figures 10 and 11.
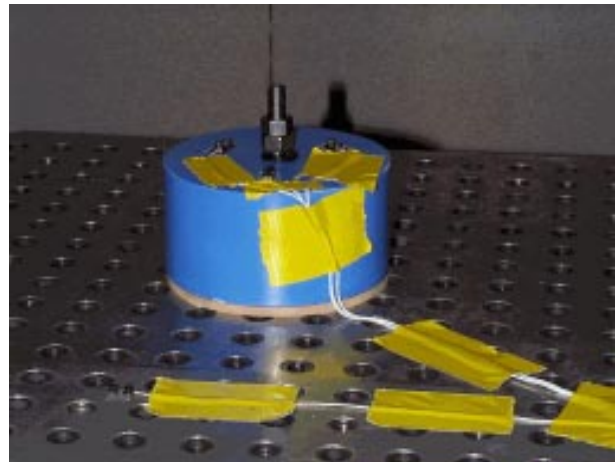
Figure 9. LANL impact test setup.

Typical accelerations measured during the impact tests are depicted in Figures 10 and 11. Both data sets are generated by dropping the carriage from an initial height of 13 inches (0.33 meters). The response of a 1/4 inch-thick (6.3 mm) layer of foam is shown in Figure 10 and the response of a 1/2 inch-thick (12.6 mm) layer is shown on Figure 11. It can be observed that over a thousand g's are measured on top of the impact cylinder which yields large deformations in the foam layer. The time scale also indicates that the associated strain rates are important. Lastly, the variation of peak acceleration observed in Figure 10 suggests that a non-zero angle of impact is involved, making it necessary to model this system with a 3D discretization. Clearly, modal superposition techniques would fail modeling this system because 1) contact can not be represented efficiently with mode shapes; 2) nonlinear hyperfoam models are needed to represent the foam's hardening behavior; and 3) very refined meshes would be required to capture the frequency content well over 10,000 Hertz.

3.2.3. Variability of the Experiment

Table 1 gives the number of data sets collected for each configuration tested. The reason why less data sets are available at high impact velocity is because these tests proved to be destructive to the elastomeric material and could not be repeated. Figure 12 shows the variability observed during the impacts when the same configuration of the system (same sample of elastomeric material and impact velocity) is tested ten times.

Table 1. Data collected with the impact testbed.

Number of Data Sets Collected	Low Velocity Impact (13 in. Drop)	High Velocity Impact (155 in. Drop)
Thin Layer (0.25 in.)	10 Tests	5 Tests
Thick Layer (0.50 in.)	10 Tests	5 Tests

Figure 10. Accelerations measured during a low-velocity impact on a thin foam layer.
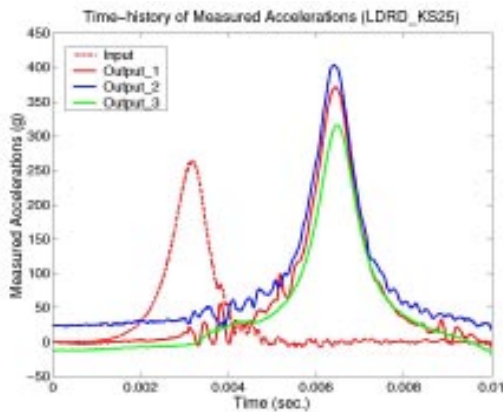
Figure 11. Accelerations measured during a low-velocity impact on a thick foam layer.
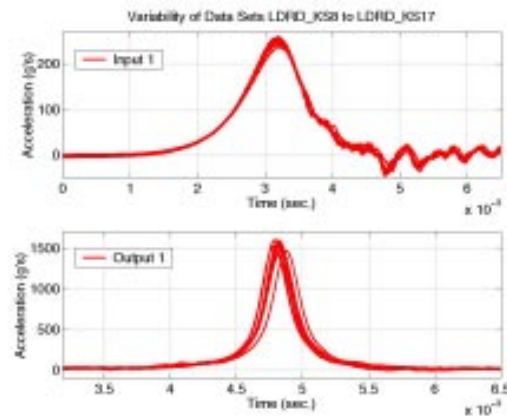
Figure 12. Accelerations measured during 10 "similar" impact tests (top: input; bottom: output 1).

Although the environment of this experiment was very well controlled, a small spread in both input and output signals is obtained. This justifies our point that model correlation and model validation must be formulated as statistical pattern recognition problems. From Figure 12, the variability of the test data can be assessed and represented in a number of ways, an illustration of which is provided in Figure 13. It shows the peak acceleration probability density functions (PDF) for each measurement. Such representation tells us, for example, that 17% of the values measured at output sensor 1 are equal to 1,520 g's when similar experiments are repeated. According to Figure 13, this value is the most probable peak acceleration. What is therefore important is that the correlated models predict

the acceleration levels with the same probability of occurrence as the one inferred from test data.
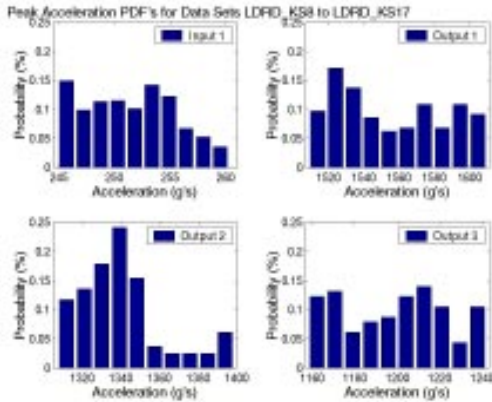
Figure 13. Probability density functions of the peak acceleration measured during 10 impact tests.

4. DIRECT CORRELATION OF TIME SERIES

One major difficulty of time-domain model validation is the reconstruction of continuous solution fields during the optimization. This issue is fundamental because, if the inverse problem is not formulated correctly, the optimized, numerical model yields discontinuous acceleration, velocity and displacement fields which contradicts the laws of mechanics for the class of problems investigated here.

With the conventional approach for solving inverse problems, parametric optimization is formulated by selecting a test-analysis correlation metric denoted by the vector {R} in equation (1). Implementing successive optimizations produces several optimized models, one for each time window considered. This is necessary not only for computational purposes but also because some of the parameters being optimized may vary in time and following such evolution as it is occurring may be critical to model validation. However, nothing in the formulation of the inverse problem enforces continuity between the solution fields obtained from models optimized within the i-th and (i+1)-th time windows. Since the design variables can converge to different solutions in successive time windows, the discontinuity of the solution can be written, for example, in terms of the displacement field as

$$\lim_{\substack{t \to t_i \\ t \le t_i}} x(p^{(i)}, t) \ne \lim_{\substack{t \to t_i \\ t \ge t_i}} x(p^{(i+1)}, t) \qquad (2)$$

The only solution currently available is to re-formulate the inverse problem as a constrained optimization where the continuity of the solution field is enforced explicitly. This strategy is based on the theory of optimal control and it relies on the resolution of multiple two-point boundary value problems (BVP).[8,9] When satisfactory solutions of the two-point BVP's are obtained, the numerical model is guaranteed to match the measured data at the beginning and at end of the time window considered. In addition, a parametric adjustment can be brought to the model to improve the correlation with test data and a non-parametric residue is best-fitted that can be used for identifying any nonlinearity, source of variability or modeling error not accounted for by the model. We emphasize that the idea of optimal error control is not original. Full credit must be given to the authors of References 8 and 9 although their original motivation was somewhat different.

Our application of this technique to a single degree of freedom system and a four-degree of freedom system shows that the optimal control approach does indeed resolve the discontinuity. This improvement comes with the additional cost of formulating a two-point BVP to guaranty continuity of the solution. Since the procedure is embedded within an optimization solver, multiple two-point BVP's must be solved for. Unfortunately, the impact on the computational requirement is enormous and practical applications currently remain out-of-reach. (Typically, identifying an unknown nonlinear force with a single degree of freedom, Duffing oscillator may require up to 20 hours of CPU time on a workstation.) For this reason, we adopt the approach of replacing the resolution of inverse problems with multiple forward, stochastic calculations.

5. VALIDATION OF NUMERICAL MODELS

Even though model updating and health monitoring have been prolific fields of research for many years, their applications have mostly been restricted to linear systems that can be accurately described by a subset of low-frequency modes. Modal-based techniques become rapidly obsolete when systems are subjected to high-frequency excitation, when variability is an issue of concern or when the dynamics of interest is strongly nonlinear. In the remainder, several issues are discussed that, we believe, are critical to the success of model validation. They are the following ones:

- Extracting features from the data;
- Developing fast probability integration tools;

- Solving stochastic optimization problems;
- Assessing the statistical consistency of data sets.

After a short discussion of the basic concepts of model validation (Section 5.1) and a description of the overall computational procedure (Section 5.2), these four issues are addressed in Sections 5.3 to 5.6.

5.1. BASIC CONCEPTS

The "philosophy" presented here is to replace the formulation of inverse problems by a methodology where error surfaces are generated from the resolution of a large number of forward, stochastic analyses, then, optimized to identify the source of modeling error. This is the only alternative to the correct yet computationally impractical formulation discussed briefly in Section 4. Besides having to account for uncertain inputs, imperfect material characterization and modeling errors during a design cycle, the other reason for this approach is to recast model updating as a problem of hypothesis testing. When the predictive quality of a model is assessed, we believe that three fundamental questions must be answered:

- Are results from the experiment(s) and simulation(s) consistent statistically?
- What is the degree of confidence associated with the first answer?
- If additional data sets are available, by how much does the confidence increase?

Hypothesis testing permits to answer these questions. The difficulty however is to assess the minimum amount of data necessary to formulate a meaningful test and to implement such a test for large-scale, numerical simulations. Although hypothesis testing is well-known, very little literature is available on the subject of "population versus population" testing. Moreover, applying conventional tools to the multivariate case is not immediate.

5.2. OVERVIEW OF THE PROCEDURE

According to the procedure illustrated in Figure 14, optimization parameters and random variables are first defined. Multiple FE solutions and multi-dimensional error surfaces are generated from statistical sampling. Error surfaces provide a metric for test-analysis correlation and model updating. The first useful tool is sensitivity analysis employed to reduce the subset of potential optimization variables down to the most

sensitive ones. Then, the best possible model is sought after through the optimization of its design parameters. When these consist of random variables, the procedure must either search for the most likely values (case where distributions are known) or optimize the statistics (case where distributions are somewhat unknown). Finally, Figure 14 shows that, rather than comparing response levels, the ability of a probabilistic model to reproduce test data must be assessed using the response's statistics.
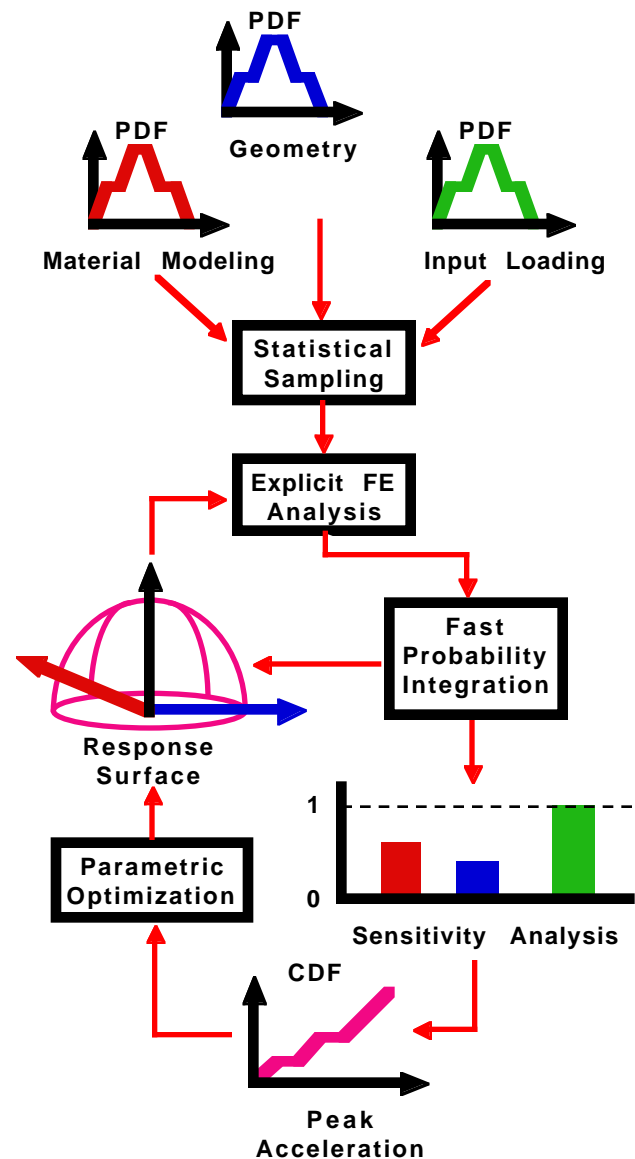
Figure 14. Flow chart showing the successive steps of model validation.

Software integration is an important part of the procedure described previously. Three software packages

American Institute of Aeronautics and Astronautics

involving four different programming languages are interfaced. The test-analysis correlation procedure is controlled by a library of Matlab functions.[10] The reason for this choice is flexibility and the possibility to develop a user graphical interface easily. Depending on the type of analysis requested by the user, the Matlab-based software writes and compiles Fortran77 routines that are used for generating the Abaqus input deck. Drivers written in the script language Python are also generated and used for piloting the FE analyses.[11] Finally, results are uploaded back into Matlab for test-analysis correlation and parametric optimization. This architecture should enable the interfacing in the near future of a variety of engineering analysis software, including parallel FE processing packages for running large-dimensional, nonlinear engineering simulations on high-performance computing platforms.

5.3. DATA CORRELATION METRICS

Large computer simulations tend to generate enormous amounts of output that must be synthesized into a small number of indicators for the analysis. This step is referred to as data reduction or feature extraction in the literature. These features are typically used to define the test-analysis correlation metrics that may be optimized depending on the predictive quality of the model. The main issue in feature extraction is to define indicators that provide meaningful insight regarding the ability of the model to capture the dynamics of the system investigated. Some of the features defined for nonlinear structural dynamics are reviewed.

- **RMS error of time series:**

The simplest of test-analysis correlation metrics is the difference between measured and predicted time series. Equation (3) shows the RMS error between peak acceleration responses cumulated over several sensors. The total simulation error is defined in equation (4).

$$J(p) = \sum_{s,sensor} \left(\ddot{x}_{measured,s}^{peak} - \ddot{x}_s^{peak}(p) \right)^2 \quad (3)$$

$$J(p) = \sum_{s,sensor} \sum_{t,time} \left(\ddot{x}_{measured,s}(t) - \ddot{x}_s(p;t) \right)^2 \quad (4)$$

- **Principal component decomposition:**

The principal component decomposition (PCD) is a comparison of manifolds.[12] Instead of comparing the signals directly, the angles between the "nonlinear subspaces" spanned by the responses are estimated. To do so, time responses are collected into data matrices whose singular value decomposition efficiently compares multi-dimensional data sets with automatic normalization. The PCD metric may be defined as

$$J(p) = \sum_i \sum_j \left(\Delta U_{ij} \right)^2 + \sum_i \Delta \sigma_i^2 + \sum_i \sum_j \left(\Delta V_{ij} \right)^2 \quad (5)$$

In equation (5), $[\Delta U]$, $\{\Delta \sigma\}$ and $[\Delta V]$ represent normalized differences between the singular values and vectors of the analysis and test data matrices defined as

$$\begin{bmatrix} \ddot{x}_1(p;t_1) & \cdots & \ddot{x}_1(p;t_m) \\ \vdots & \ddots & \vdots \\ \ddot{x}_n(p;t_1) & \cdots & \ddot{x}_n(p;t_m) \end{bmatrix} = [U(p)][\Sigma(p)][V(p)]^T \quad (6)$$

$$[\Delta U] = \left([U_{test}]^T [U(p)] - [I] \right) \quad (7)$$

$$[\Delta V] = \left([V_{test}]^T [V(p)] - [I] \right) \quad (8)$$

$$[\Delta \Sigma] = [\Sigma_{test}]^{-1} \left([\Sigma_{test}] - [\Sigma(p)] \right) \quad (9)$$

Although more computationally intensive, this feature provides an elegant framework for interpreting the data by generalizing the notion of mode shapes and modal contributions to nonlinear systems. It may also filter out measurement noise that is typically associated with small singular values.

- **Shock response spectrum:**

The shock response spectrum (SRS) is obtained by calculating the response of a single degree of freedom system to a known input such as, for example, the acceleration signal denoted by I(t) below. The response is then characterized by a given criterion. For example, an acceleration spectrum is defined by plotting

$$SRS_s(\omega) = \ddot{x}_s^{peak}(\omega) \quad (10)$$

versus ω, the system's frequency after the acceleration response has been obtained by integrating the equation

$$\ddot{x}(t) + 2\zeta\omega\dot{x}(t) + \omega^2 x(t) = I(t) \quad (11)$$

The purpose of SRS analysis is to avoid selecting modal characteristics that may result into significant response levels when designing a sub-component. A correlation metric based on SRS data is defined as

$$J(p) = \sum_{s,sensor} \sum_{i,design} \left(SRS_{test,s}(\omega_i) - SRS_s(p;\omega_i) \right)^2 \quad (12)$$

The advantage of the previous three features (RMS error, PCD and SRS) is that no assumption is made regarding the dynamics encountered. They apply to linear and nonlinear systems alike. The remaining features presented below assume specific model forms, from first-order to second-order representations. Thus, they are relevant to the analysis of linear systems only.

- **ARMA-based features:**

An auto-regressive, moving average (ARMA) model can always be best-fitted to the data, whether the system is linear or not. To do so, coefficients of the following linear combination are calculated

$$\ddot{x}_s(t) = \sum_{i=1\cdots N_{AR}} \alpha_{si} \ddot{x}_s(t - i\Delta t) + \sum_{j=1\cdots N_{MA}} \beta_{sj} F_s(t - j\Delta t) \quad (13)$$

Coefficients of the models obtained from test and analysis data can be compared to define the correlation metric. Another possibility is to employ the coefficients obtained by fitting the test data to predict the simulation response and to estimate the error between the predicted and actual simulation responses. These alternatives are illustrated in equations (14) and (15), respectively

$$J(p) = \sum_{s,sensor} \sum_{i,order} \left(\alpha_{test,si} - \alpha_{si}(p) \right)^2 \quad (14)$$

$$J(p) = \sum_{s,sensor} \sum_{t,time} \left(\ddot{x}_s(p;t) - \hat{\ddot{x}}_s(t) \right)^2 \quad (15)$$

- **Frequency response functions:**

The frequency response function (FRF) of a linear system is defined as the inverse of the dynamic stiffness matrix at a given forcing frequency Ω

$$[H(\Omega)] = \left([K] + j\Omega[D] - \Omega^2[M] \right)^{-1} \quad (16)$$

Equation (16) constitutes the basic tool for calculating a model's FRF data between specified input and output locations. Similarly, a system's FRF can be identified from measurements by dividing the cross-correlation function of a given input-output pair by the input's auto-correlation function. The RMS error between the two sets of FRF curves can be formed as another metric for test analysis correlation

$$J(p) = \sum_{ij,sensor} \sum_{k,frequency} \left(H_{measured,ij}(\Omega_k) - H_{ij}(p;\Omega_k) \right)^2$$
$$(17)$$

- **ERA-based features:**

Finally, a second-order, linear model can be formulated by representing the input-output, FRF data as a superposition of modal contributions

$$H_{ij}(\Omega) = \sum_{k,mode} \frac{\Phi_{ik}\Phi_{jk}}{\omega_k^2 + 2j\zeta_k\omega_k\Omega - \Omega^2} \quad (18)$$

Numerous algorithms are available for time-domain or frequency-domain system identification among which we cite the Eigensystem Realization Algorithm (ERA).[13] Its advantage is that it can be automated to a large amount to extract the resonant frequencies ω_k, modal damping ratios ζ_k and mode shapes $\{\Phi_k\}$ directly from the measured or predicted time signals. Then, various metrics can be defined as

$$J(p) = \sum_{k,mode} \left(\frac{\omega_{test,k}^2 - \omega_k^2(p)}{\omega_{test,k}^2} \right)^2 \quad (19)$$

$$J(p) = \sum_{k,mode} \left(\frac{\zeta_{test,k} - \zeta_k(p)}{\zeta_{test,k}} \right)^2 \quad (20)$$

$$J(p) = \sum_{s,sensor} \sum_{k,mode} \left(\Phi_{test,sk} - \Phi_{sk}(p) \right)^2 \quad (21)$$

Figure 15 compares the six metrics defined by equations (4), (5), (12), (15), (17) and (19) for test-analysis correlation based on RMS error, PCD, SRS, ARMA, FRF and ERA features, respectively. This illustration is provided with the 8-DOF testbed because its measured responses are difficult to characterize (see Figure 6 where responses look like random, zero-mean signals). Assessing the predictive quality of a numerical simulation is therefore a difficult task.
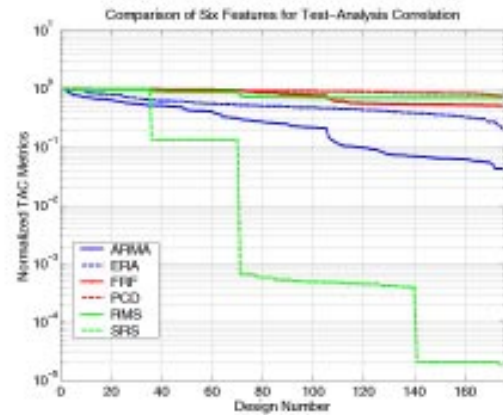
Figure 15. Comparison of various features used to refine the explicit FE model of the 8-DOF system.

In Figure 15, the horizontal axis represents 175 designs evaluated and compared to the test data during a parametric optimization procedure. The objective is to identify the best possible friction model. Here, "best model" refers to a design that minimizes a particular test-analysis correlation metric. It can be observed that only the SRS-based metric (12) segregates "good" from "poor" designs. This illustrates the importance of feature selection for test-analysis correlation and optimization.

5.4. FAST PROBABILITY INTEGRATION

Fast probability integration (FPI) is used to propagate efficiently variability information during structural analysis. Our FPI capability relies on NESSUS (which stands for Numerical Evaluation of Stochastic Structures Under Stress), a software for analyzing the reliability of mechanical systems that provides a practical way of propagating uncertainty throughout the calculations.[14] Using a software package for reliability analysis to address test-analysis correlation is achieved by following the steps detailed below.

First, it is assumed that the model's random variables collected in a vector $\{X\}$ are defined. These may include uncertain input forces, random parameters for material modeling, manufacturing tolerances, etc. We also define a response function Z and the objective of the FE calculation is to estimate the value of Z for a given sample $\{X\}$ of our random variables. Finally, a limit state function $g(X)$ is defined that describes the correlation with test data. "Success" is defined if $g(X)=0$, that is, if the response measured during the test is matched by the model in a probabilistic sense. It means that the problem of model validation consists of calculating the PDF or the cumulative density function (CDF) of the Z-response, respectively defined as

$$p_Z(\alpha) = \text{Prob}[Z = \alpha]$$
$$F_Z(\alpha) = \text{Prob}[Z \le \alpha] = \int_{-\infty}^{\alpha} p_z(z)dz \quad (22)$$

The central aspect of FPI is the search for the most probable prediction (MPP) of the model in the presence of uncertainty. To obtain the MPP, the Z-response's joint PDF is maximized under the constraint $g(X)=0$. This optimization is solved by converting the original variables $\{X\}$ into standardized normal variables $\{u\}$, that is, variables described by the unit normal CDF

$$\Phi(u) = \int_{-\infty}^{u} \frac{1}{\sqrt{2\pi}} e^{-\frac{s^2}{2}} ds \quad (23)$$

Once the MPP has been determined, the response surface can be explored to reconstruct the entire PDF or CDF. The transformation from $\{X\}$ to $\{u\}$ and its inverse are achieved using the Rosenblatt transform[15]

$$u = \Phi^{-1}(F_Z(X)), \quad X = F_Z^{-1}(\Phi(u)) \quad (24)$$

An illustration is presented with the impact testbed discussed in Section 3.2. For this application, several 2D and 3D models are developed. Among the parameters varied are the type of elements used in the discretization; the size of the mesh; the type of contact conditions implemented; the material modeling; the preload applied when the center bolt is tightened; the angles of the steel impactor at impact; and the input acceleration. The two types of information obtained by FPI are illustrated in Figures 16 and 17. Here, we are interested in predicting the probability distribution of the peak acceleration at output sensor 1 at the time of impact. From Figure 16, it can be seen, for example, that the probability that the peak acceleration be less than 1,520 g's is equal to 90%.
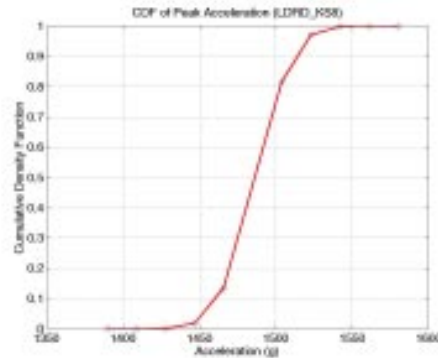
Figure 16. CDF of the peak acceleration predicted by numerical simulation of the impact test.
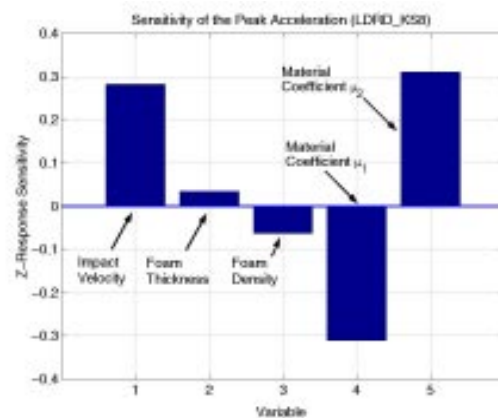
Figure 17. Sensitivity of the CDF with respect to various random, design parameters.

The second type of information obtained from FPI is sensitivity data for comparing the influence of each random variable. Figure 17 summarizes a study where the influence of five variables (impact velocity, foam thickness, foam density and parameters of the stress-strain, hyperfoam model) is investigated.

5.5. OPTIMIZING STOCHASTIC MODELS

In this Section, we discuss results obtained when the explicit, nonlinear FE simulations are optimized to match test data. The illustration provided in the remainder involves the impact testbed. When correlation with test data is not satisfactory, Z-response surfaces are used to generate fast-running models. These, in turn, provide the core of the parametric optimization algorithm that fine-tunes a subset of the model's design variables to improve the correlation with test data.

Figure 18 pictures a typical Z-response surface obtained with the 3D model: the two horizontal axes represent the values spanned by two parameters and the vertical axis represents the PCD cost function (5) on a log scale. For clarity, the surface is shown as only two of the seven optimization variables are varied. The complete set includes two coefficients of the hyperfoam material model; two angles of impact that simulate a small free-play in the alignment of the carriage and steel impactor; the bolt preload; the input acceleration scaling factor; and a numerical bulk viscosity parameter. A total of 1,845 FE models are analyzed to generate a fast-running model after having determined the approximate location of the MPP from probabilistic analysis.
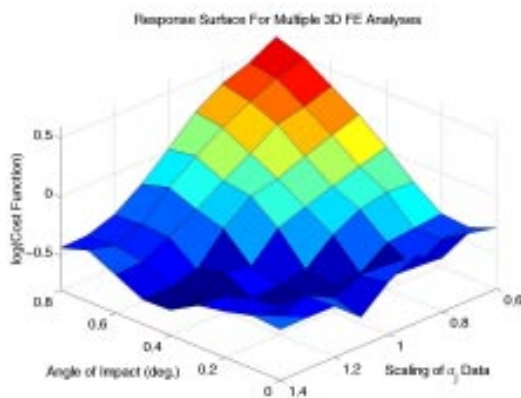
Figure 18. Z-response surface. (The metric defined is the PCD cost (5) based on three accelerations.)

Figure 19 depicts the correlation before and after parametric optimization. A clear improvement of the

model's predictive quality is witnessed which, in turn, leads to a more accurate representation of the viscoelastic material. Note that the metric employed for optimizing the parameters (PCD, shown in Figure 18) is different from the correlation metric that consists in comparing the time-domain, acceleration signals. One difficulty is that of determining the optimal distribution of an input, random variable. An analyst may be faced with this problem when no a priori information is available regarding the definition of a variable. The optimization of unknown distributions is still, to the best of our knowledge, an area of open research. Subjective probability and Bayesian belief network may resolve this difficulty.[16] They define an attractive framework for assessing the influence of prior distributions on posterior, test-analysis correlation indicators.
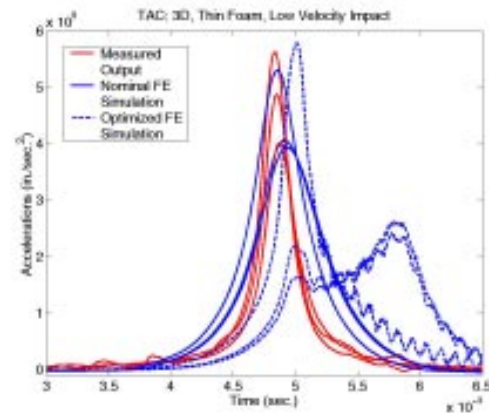
Figure 19. Correlation of the 3D model.

The last aspect of model validation addressed in this Section consists of verifying that the optimized model is indeed correct. This is achieved by comparing predictions of various models to measured data sets for configurations different from the one used during FPI and optimization. For example, the 3D models are optimized using the thin pad/low impact velocity setup. Then, the 2D, axi-symmetric models are verified with the thick pad/low impact velocity setup.

On Figure 20, predictions of the original and final 2D models are compared to test data measured during a low-velocity impact using the 0.25 in. (6.3 mm) thick foam pad. On Figure 21, the response of a 0.50 in. (12.6 mm) thick foam pad is shown. Despite small oscillations attributed to numerical noise generated by the contact algorithm, the models predict the acceleration levels measured during the test. We believe that these independent checks constitute the only valid indication that the modeling is correct.
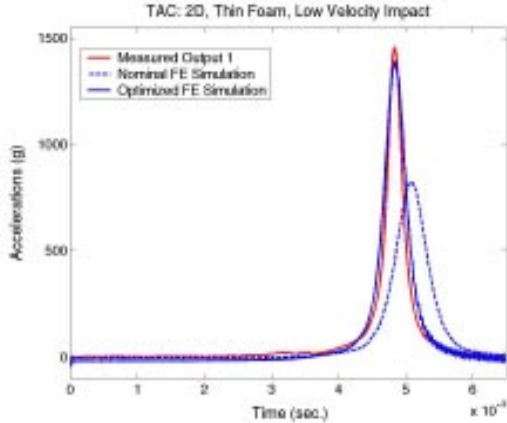
Figure 20. Verification of the predictions: Response of a thin pad (1/4 in., 6.3 mm).
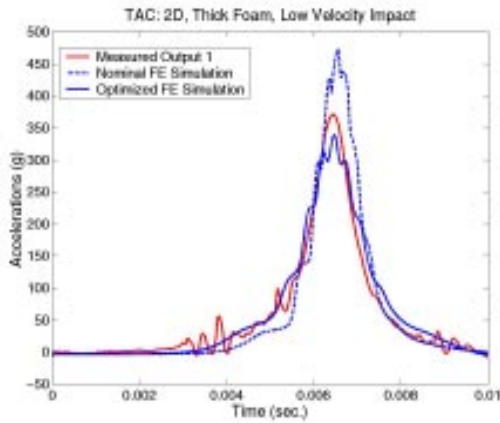
Figure 21. Verification of the predictions: Response of a thick pad (1/2 in., 12.6 mm).

5.6. STATISTICAL HYPOTHESIS TESTING

One of the open research issues that this work has identified is the problem of establishing a correlation between multiple data sets. By this we mean "assessing the degree to which two populations are consistent with each other." Our literature review seems to indicate that tools for assessing the distance between multiple data sets are not readily available in the context of statistical correlation and multivariate analysis.

This difficulty is illustrated in Figure 22. It shows the peak acceleration values for channels 1 and 2 of the impact testbed plotted against each other. The data of ten independent, "identical" tests are shown together with simulation results from two different models. For each one of the two models, a particular design is generated by varying the angles of impact and the bolt preload. Then, each design is analyzed using the ten different

input acceleration signals measured. The three ellipsoids shown in Figure 22 illustrate the 95% confidence intervals for the test data and two models. The predictive quality of one of the models is better because most of its data points (68 of 100) fall within the 95% confidence interval of the test data. The other model predicts 34 of 100 points within the test's 95% confidence interval.
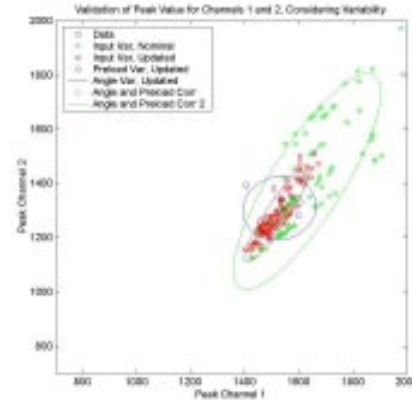
Figure 22. Comparison of test and analysis data in a two-feature space. (The 2D space represents the peak accelerations measured or predicted at sensors 1 and 2.)

By inspection of Figure 22, it is apparent that the peak magnitudes of measured accelerations 1 and 2 are uncorrelated because the 95% confidence interval is nearly circular. Thus, we suspect that one of the greater sources of variability is the source that affects the channels differently. This conclusion, however, is not confirmed by data generated from the two models. A better illustration is provided in Figure 23 where the joint CDF interpolated from test data is compared to CDF's of the two models. It illustrates the disagreement between test data and simulations.
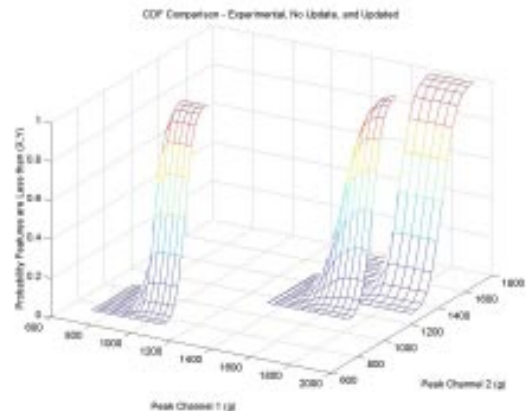
Figure 23. Comparison of cumulative density functions for the test data and two simulations.

This example illustrates that plotting several features against each other defines a powerful analysis tool. Unfortunately, higher-order graphics are difficult to represent, therefore, requiring quantitative indicators of the model's fit to test data. Such statistical consistency can be assessed using a standard, multivariate Hotelling's T^2 test. First, statistics are calculated from the distributions of features. In the following, the vectors of mean values are denoted by $\{\mu\}$ and covariance matrices are denoted by $[\Sigma]$. Hotelling's T^2 test states that the mean vector of the model features is an estimate of the mean vector of test features to the $(100-\alpha)\%$ confidence level if

$$\left(\{\mu(p)\} - \{\mu_{test}\}\right)^T \left[\Sigma_{test}\right]^{-1}\left(\{\mu(p)\} - \{\mu_{test}\}\right) \tag{25}$$
$$\leq \frac{N_p\left(N_s - 1\right)}{N_s\left(N_p - 1\right)} F_{N_p, N_s - N_p}(\alpha)$$

Applied to the data shown in Figures 22-23 and characterized by $N_p = 2$ features and $N_s = 100$ samples, the statistics (25) sets the acceptance ratio to 1.0035 at the 95% confidence level. The Mahalanobis distance in the left-hand side of equation (25) is equal to 4.0 for the first model which clearly indicates that it fails the test. The Mahalanobis distance of the second model is equal to 0.2. This establishes that the mean response predicted by our second model has converged. It can alternatively be stated that we are 95% certain that the average peak accelerations predicted by this model are consistent with test data given the sources of variability of the experiment and given the sources of uncertainty of the model. However, this conclusion remains of limited practical use for model validation as long as the variance of the population has not converged as well.

One of the only possibility available for testing both mean and variance is to calculate Kullback-Leibler's relative entropy defined as the expected value of the ratio between the PDF's of the two populations

$$I(Model \| Test) = E\left[\frac{p_Z^{model}(\alpha)}{p_Z^{test}(\alpha)}\right] \tag{26}$$

If the features used $\{Z\}$ are normally distributed or if enough data points are available to justify the application of the central limit Theorem, the relative entropy can be approximated using Gaussian PDF's to represent the test and analysis distributions. Then, this entropy may be used for assessing the consistency between two populations of features and for optimizing parameters of a statistical model. We emphasize that the

computational requirement associated to this procedure may become important since the probability distribution of each feature considered for test-analysis correlation must be assessed for each candidate design evaluated during the optimization. This, however, is the only possibility to guaranty at a given confidence level that the numerical simulation is validated in the context of uncertainty propagation. For all practical purposes, the normal approximation to definition (26) is stated as

$$I(Model \| Test) \cong \frac{1}{2} Trace\left(\left[\Sigma(p)\right]\left[\Sigma_{test}\right]^{-1}\right) \tag{27}$$
$$-\frac{1}{2}N_p - \frac{1}{2}\log\left(\frac{\det[\Sigma(p)]}{\det[\Sigma_{test}]}\right)$$
$$+\frac{1}{2}\left(\{\mu(p)\} - \{\mu_{test}\}\right)^T \left[\Sigma_{test}\right]^{-1}\left(\{\mu(p)\} - \{\mu_{test}\}\right)$$

An illustration is provided in Figure 24 where the value of the Kullback-Leibler entropy is represented with four different models (the original material model of the impact testbed and three others obtained after successive optimization steps). Almost two orders of magnitude are obtained between the entropy of the original and final models. It demonstrates the efficiency of this statistical indicator for characterizing the predictive quality of a model based on multivariate data features.
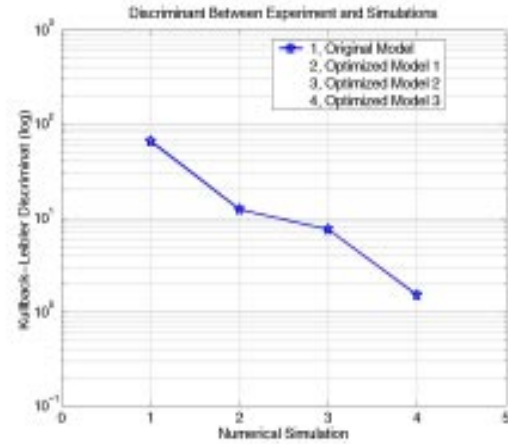
Figure 24. Evolution of the Kullback-Leibler entropy when optimizing the hyperfoam material.

Unfortunately, statistical tests for verifying a pass/fail hypothesis based on the relative entropy (27) are not available in the general case. This limitation is currently being addressed by investigating the efficiency of conventional hypothesis testing.

CONCLUSION

In this publication, a general framework is proposed for validating numerical models for nonlinear, transient dynamics. To bypass difficulties identified when applying test-analysis correlation methods to nonlinear vibration data, inverse problems are replaced with multiple forward, stochastic problems. After a metric has been defined for comparing test and analysis data, response surfaces are generated that can be used for assessing in a probabilistic sense the quality of a particular simulation with respect to "reference" or test data and for optimizing the model's design parameters to improve its predictive quality. Data sets from several experiments conducted at Los Alamos National Laboratory in support of our code validation and verification program are used to illustrate the advantages and drawbacks of this approach. Several directions of research are stated throughout this work. One of them is to implement methods of statistical, hypothesis testing to assess the consistency between test data and numerical simulations using multivariate test-analysis correlation. Combining the parametrized uncertainty approach with the estimation of the experiment's total uncertainty is also a direction that may be pursued in the future. Finally, we mention the demonstration of the entire procedure with a complex experiment during which nonlinear, structural systems are subjected to transient, explosive loading.

REFERENCES

[1] Belvin, W.K., "Second-Order State Estimation Experiments Using Acceleration Measurements," *AIAA Journal of Guidance, Control and Dynamics*, Vol. 17, No. 1, Jan.-Feb. 1994, pp. 97-103.

[2] Doebling, S.W., Farrar, C.R., Prime, M.B., Shevitz, D.W., "Damage Identification and Health Monitoring of Structural and Mechanical Systems From Changes in Their Vibration Characteristics: A Literature Review," *Report #LA-13070-MS, Los Alamos National Laboratory*, Los Alamos, NM, May 1996.

[3] Hemez, F.M., Doebling, S.W., "Test-Analysis Correlation and Finite Element Model Updating For Nonlinear, Transient Dynamics," *17th SEM International Modal Analysis Conference*, Kissimmee, FL, Feb. 8-11, 1999, pp. 1501-1510.

[4] Hemez, F.M., Doebling, S.W., "Validation of Nonlinear Modeling From Impact Test Data Using Probability Integration," *18th SEM International Modal Analysis Conference*, San Antonio, TX, Feb. 7-10, 2000, to be published.

[5] Hemez, F.M., Doebling, S.W., "A Validation of Bayesian Finite Element Model Updating For Linear Dynamics," *17th SEM International Modal Analysis Conference*, Kissimmee, FL, Feb. 8-11, 1999, pp. 1545-1555.

[6] Abaqus/Explicit User's Manual, Version 5.8, Hibbitt, Karlsson & Sorensen, Pawtucket, RI, 1997.

[7] **Instruction Manual For the Lansmont Model 610 Shock Test Machine**, Version 1.0 KJG, Lansmont Corp., Pacific Grove, CA.

[8] Mook, D.J., "Estimation and Identification of Nonlinear Dynamic Systems," *AIAA Journal*, Vol. 27, No. 7, July 1989, pp. 968-974.

[9] Dippery, K.D., Smith, S.W., "An Optimal Control Approach to Nonlinear System Identification," *16th SEM International Modal Analysis Conference,* Santa Barbara, CA, Feb. 2-5, 1998, pp. 637-643.

[10] **Matlab**™, User's Manual, Version 5.3, The MathWorks, Inc., Natick, Massachusetts, 1999.

[11] Lutz, M., **Programming Python**, O'Reilly & Associates, Inc., 1996.

[12] Hasselman, T.K., Anderson, M.C., Wenshui, G., "Principal Components Analysis For Nonlinear Model Correlation, Updating and Uncertainty Evaluation," *16th SEM International Modal Analysis Conference*, Santa Barbara, CA, Feb. 2-5, 1998, pp. 664-651.

[13] Juang, J.N., **Applied System Identification**, Prentice Hall, Englewood Cliffs, NJ, 1994.

[14] **NESSUS**, User's Manual, Version 2.3, Southwest Research Institute, San Antonio, TX, 1996.

[15] Rosenblatt, M., "Remarks on a Multivariate Transformation," *The Annals of Mathematical Statistics*, Vol. 23, No. 3, 1952, pp. 470-472.

[16] Hanson, K.M., "A Framework For Assessing Uncertainties in Simulation Predictions," *Physica D*, Elsevier Science, May 1999, to be published.